NREL
Transforming ENERGY

U.S. DEPARTMENT OF ENERGY
Office of ENERGY EFFICIENCY & RENEWABLE ENERGY

On the Low Risk of Subsynchronous Resonance (SSR) in Type III Wind Turbines Operating in Grid-Forming Control

Authors: Weihang Yan, Shahil Shah, Vahan Gevorgian, Przemyslaw Koralewicz, Robb Wallen

Supported by US DOE Wind Energy Technologies Office

21st Wind and Solar Integration Workshop
Hague, Netherlands
Oct. 12, 2022

Outline

- Evaluation of SSR Risk in Grid-Forming Type III Wind Turbines
  - EMT Simulations
  - Experimental Impedance Measurements
- Source of SSR in Standard Grid-Following Type III Wind Turbines
- Genesis of Low Risk of SSR in Grid-Forming Type III Wind Turbines
  - Control Implementation for GFM Type III Wind Turbines
  - Sequence Impedance Models of GFM Type III Wind Turbines
- Summary

SSR in DFIG based Type III Wind Power Plants

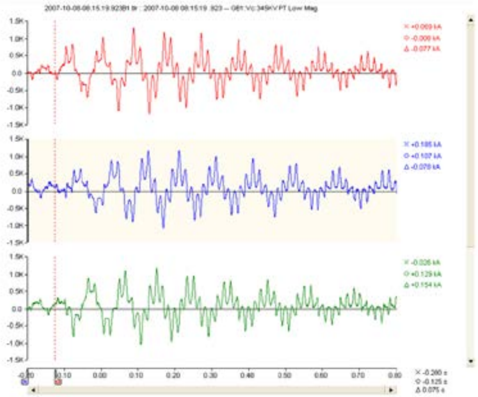

US Minnesota 2007

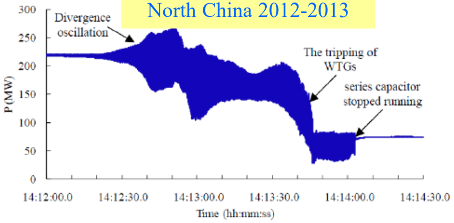

North China 2012-2013

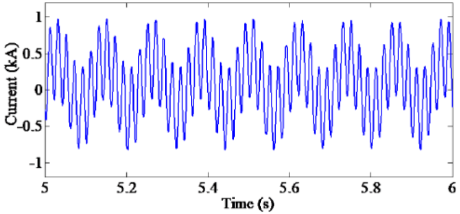

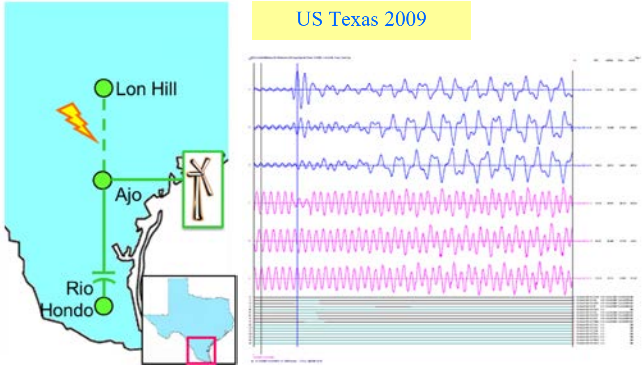

US Texas 2009

West China 2015

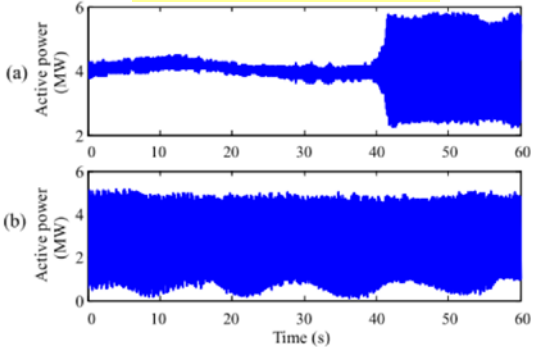

Zhangbei, China 2020

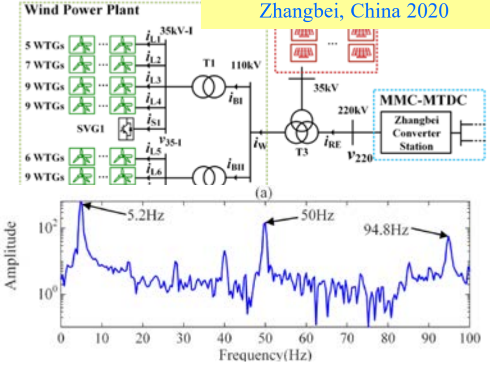

US Texas 2017

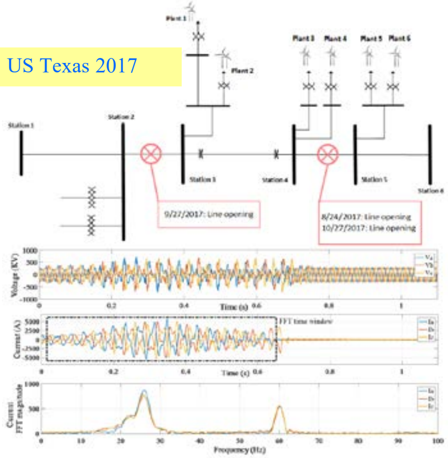

Source: Y. Cheng et al., "Real-World Subsynchronous Oscillation Events in Power Grids with High Penetrations of Inverter-Based Resources," *IEEE Trans. on Power Syst.*, Early Access.

SSR Risk in Type III Turbines for GFM vs GFL Mode

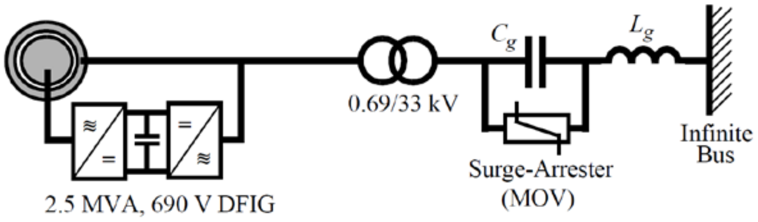

GFL Control

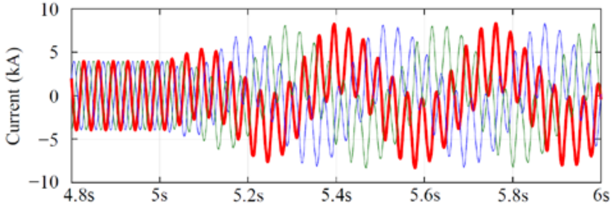

(a). Type III wind turbine in GFL control

GFM Control

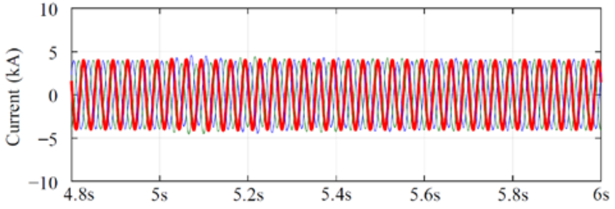

(b). Type III wind turbine in GFM control

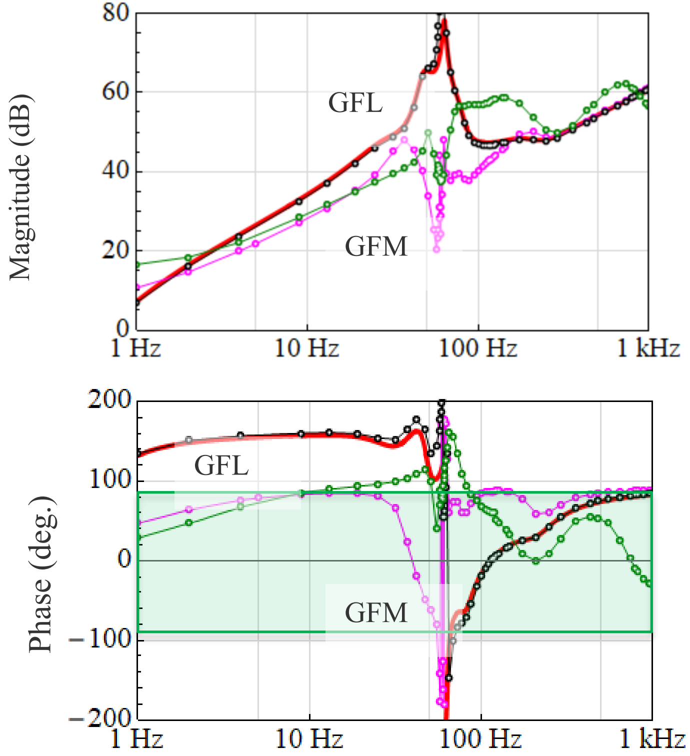

Simulation and Impedance Responses show Better Damping for GFM Control Mode

Impedance Meas. of a 2.5 MW GFM Type III Turbine

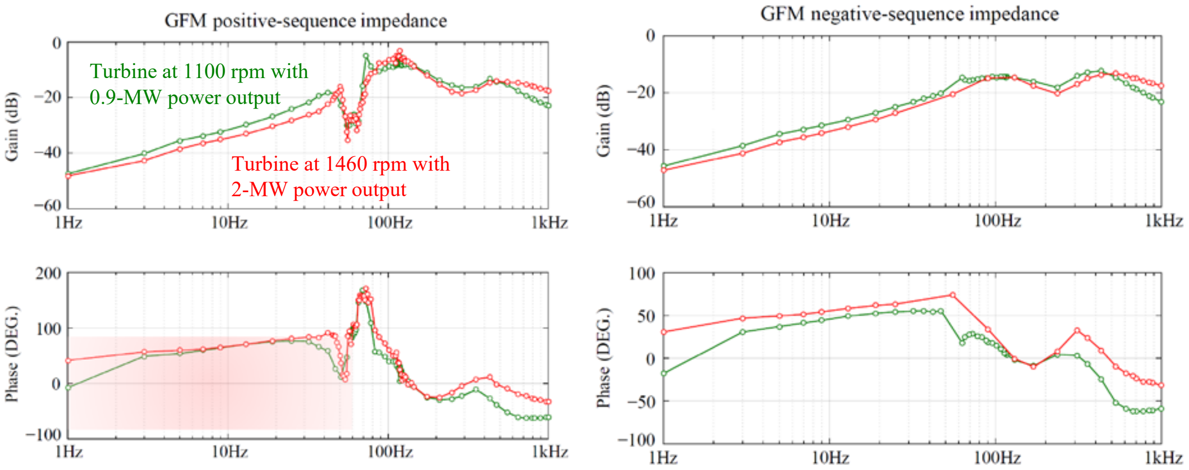

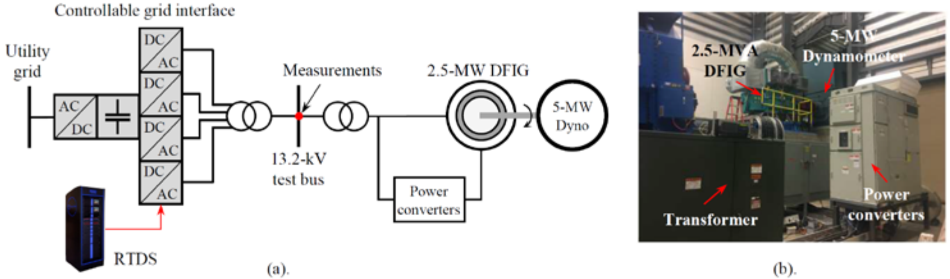

(a). (b).

Fig. 1. Test setup for the impedance measurement of the 2.5-MW Type III GFM wind turbine at NREL's Flatiron Campus: (a) measurement system schematic and (b) test photo. *Photo by NREL*

- Type III GFM wind turbines naturally exhibit positive resistance or damping in subsynchronous frequency range
- This behavior is independent of the operation condition

Source of SSR in Grid-Following Type III Turbines

- Positive Sequence Impedance Model:

$$Z_{p,\mathrm{GFL}}(s) \approx R_s + \frac{R'_r}{\sigma_p(s)} + \frac{k_m V_{\mathrm{dc}}}{\sigma_p(s)}\left(\frac{N_s}{N_r}\right)^2 k_{\mathrm{pr}} + s\left(L_{\mathrm{ls}} + L'_{\mathrm{lr}}\right) + \frac{k_m V_{\mathrm{dc}}}{\sigma_p(s)}\left(\frac{N_s}{N_r}\right)^2 \left[\frac{1}{(s - j\omega_1)T_{\mathrm{ir}}} - jK_{\mathrm{rd}}\right]$$

where: $$\sigma_p(s) = \frac{s - j\omega_m}{s}$$

The negative resistance in the impedance response is due to the interaction between the proportional gain (k_{pr}) of the RSC current controller and the dynamic slip $\sigma_p(s)$.

- Impedance response of GFL Type III Wind Turbines

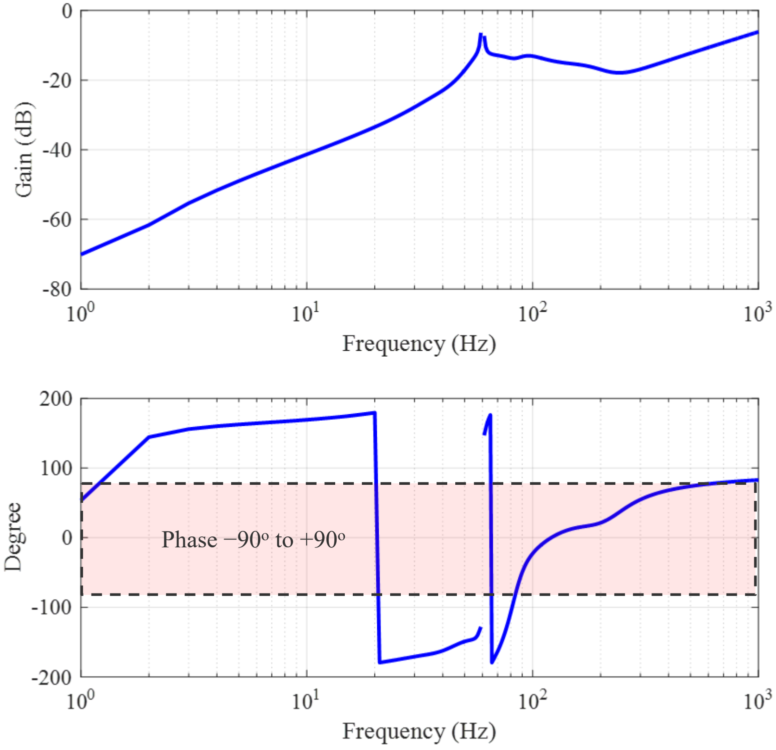

GFM and GFL Control of Type III Wind Turbines

RSC Inner-loop Control & GSC Control

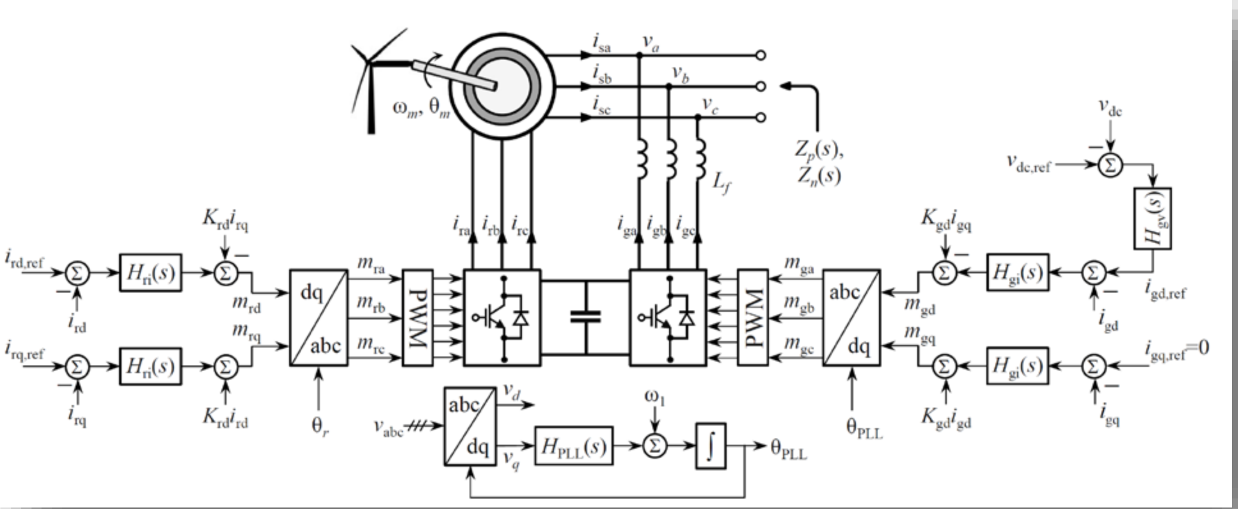

Reference: Shah, Shahil, and Vahan Gevorgian. 2020. Control, Operation, and Stability Characteristics of Grid-Forming Type III Wind Turbines: Preprint. Golden, CO: National Renewable Energy Laboratory. NREL/CP-5D00-78158. https://www.nrel.gov/docs/fy21osti/78158.pdf

Note: This slide shows generic control implementation. It does not necessarily represent control implementation in the 2.5 MW wind turbine used for experimental impedance measurements.

GFL outer-loop control:

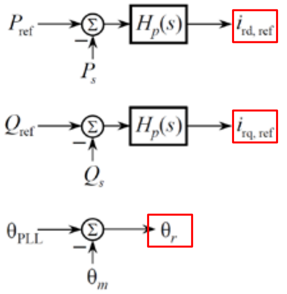

GFM outer-loop control:

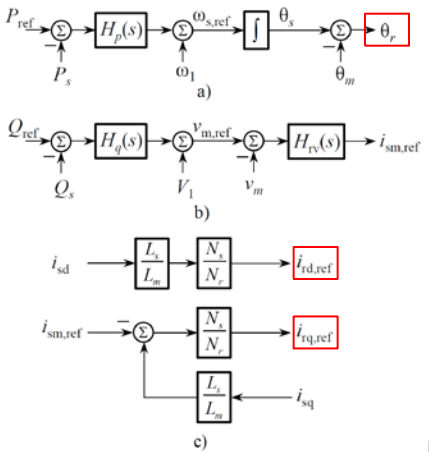

Sequence Impedance Modeling and Validation

- Positive-sequence impedance of DFIG with GFM control:

$$Z_{\mathrm{sp}}(s)=\frac{\begin{gathered}R_s+\frac{R_r'}{\sigma_p(s)}+s\left(L_{\mathrm{ls}}+L_{\mathrm{lr}}'\right)+\frac{k_m V_{\mathrm{dc}}}{\sigma_p(s)}\left(\frac{N_s}{N_r}\right)^2\left[\left(1-\frac{L_s}{L_m}\right)H_{\mathrm{ri}}(s-j\omega_1)-jK_{\mathrm{rd}}\right]\\ +j\frac{3}{4}\frac{k_m V_{\mathrm{dc}}}{\sigma_p(s)}\frac{N_s}{N_r}V_1\left[\left(\mathbf{I}_{r0}-\frac{N_s}{N_r}\frac{L_s}{L_m}\mathbf{I}_{s0}\right)H_{\mathrm{ri}}(s-j\omega_1)-j\mathbf{I}_{r0}K_{\mathrm{rd}}+\mathbf{M}_{r0}\right]T_p(s-j\omega_1)+\frac{3}{4}\frac{k_m V_{\mathrm{dc}}}{\sigma_p(s)}\left(\frac{N_s}{N_r}\right)^2 V_1 T_q(s-j\omega_1)\end{gathered}}{\begin{gathered}1-j\frac{1}{2}\frac{k_m V_{\mathrm{dc}}}{\sigma_p(s)}\left(\frac{N_s}{N_r}\right)^2 H_{\mathrm{rv}}(s-j\omega_1)H_{\mathrm{ri}}(s-j\omega_1)\\ +j\frac{3}{4}\frac{k_m V_{\mathrm{dc}}}{\sigma_p(s)}\frac{N_s}{N_r}\mathbf{I}_{s0}^{*}\left[\left(\mathbf{I}_{r0}-\frac{N_s}{N_r}\frac{L_s}{L_m}\mathbf{I}_{s0}\right)H_{\mathrm{ri}}(s-j\omega_1)-j\mathbf{I}_{r0}K_{\mathrm{rd}}+\mathbf{M}_{r0}\right]T_p(s-j\omega_1)-\frac{3}{4}\frac{k_m V_{\mathrm{dc}}}{\sigma_p(s)}\left(\frac{N_s}{N_r}\right)^2 \mathbf{I}_{s0}^{*}T_q(s-j\omega_1)\end{gathered}}$$

- Positive-sequence impedance of DFIG with GFL control:

$$Z_{\mathrm{sp}}(s)=\frac{\begin{gathered}R_s+\frac{R_r'}{\sigma_p(s)}+s(L_{\mathrm{ls}}+L_{\mathrm{lr}}')\\ +\frac{k_m V_{\mathrm{dc}}}{\sigma_p(s)}\frac{N_s}{N_r}\left\{\frac{N_s}{N_r}\left[H_{\mathrm{ri}}(s-j\omega_1)-jK_{\mathrm{rd}}\right]+\frac{3}{2}V_1 G_p(s-j\omega_1)H_p(s-j\omega_1)H_{\mathrm{ri}}(s-j\omega_1)\right\}\end{gathered}}{1-\frac{1}{2}\frac{k_m V_{\mathrm{dc}}}{\sigma_p(s)}\frac{N_s}{N_r}\left\{\mathbf{I}_{r0}\left[H_{\mathrm{ri}}(s-j\omega_1)-jK_{\mathrm{rd}}\right]+\mathbf{M}_{r0}\right\}\frac{T_{PLL}(s-j\omega_1)}{V_1}}$$

- Positive-sequence impedance of Type III wind turbines (both GFM and GFL):

$$Z_p(s)=\frac{Z_{\mathrm{sp}}(s)\cdot Z_{\mathrm{gp}}(s)}{Z_{\mathrm{sp}}(s)+Z_{\mathrm{gp}}(s)}$$

Positive-sequence impedance of GSC

Sequence Impedance Modeling Validation

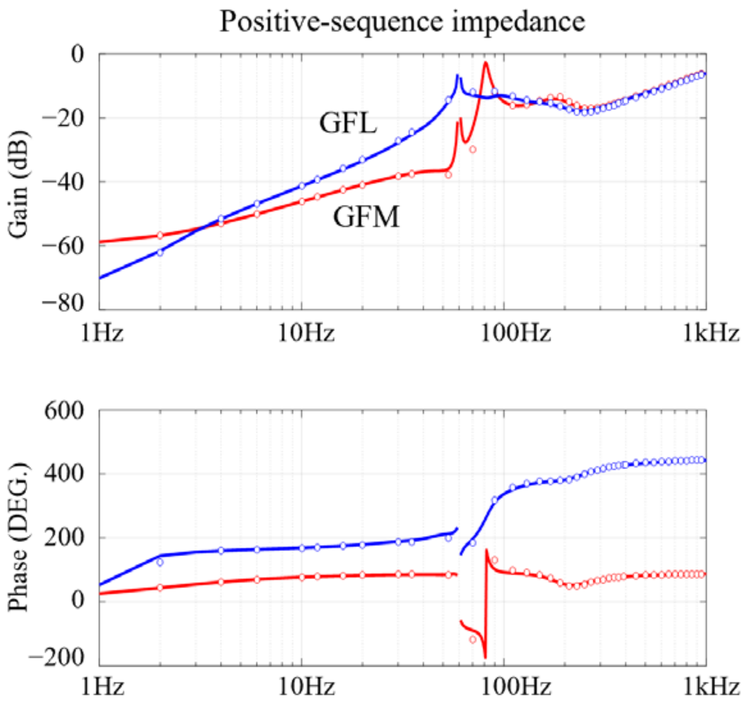

Impedance Model Reduction and Validation

Principles of Model Reduction:

- Outer-loop controls, power control and voltage control, are ignored as they are designed with much slower control bandwidths.
- Impedance of the GSC is ignored as it appears in parallel with the induction generator impedance, which is significantly smaller at low frequencies.

$$Z_{p,\mathrm{GFM}}(s) \approx Z_{p,\mathrm{GFL}}(s) - \frac{k_m V_{\mathrm{dc}}}{\sigma_p(s)} \left(\frac{N_s}{N_r}\right)^2 \frac{L_s}{L_m} H_{\mathrm{ri}}(s - j\omega_1)$$

Expand current control compensator $H_{\mathrm{ri}}(s)$

$$Z_{p,\mathrm{GFM}}(s) \approx R_s + \frac{R_r'}{\sigma_p(s)} + \frac{k_m V_{\mathrm{dc}}}{-\sigma_p(s)} \left(\frac{N_s}{N_r}\right)^2 \frac{L_{\mathrm{ls}}}{L_m} k_{\mathrm{pr}} + s\left(L_{\mathrm{ls}} + L_{\mathrm{lr}}'\right) + \frac{k_m V_{\mathrm{dc}}}{-\sigma_p(s)} \left(\frac{N_s}{N_r}\right)^2 \left[\frac{L_{\mathrm{ls}}}{L_m} \frac{1}{(s - j\omega_1) T_{\mathrm{ir}}} + jK_{\mathrm{rd}}\right]$$

Sequence Impedance Modeling Validation

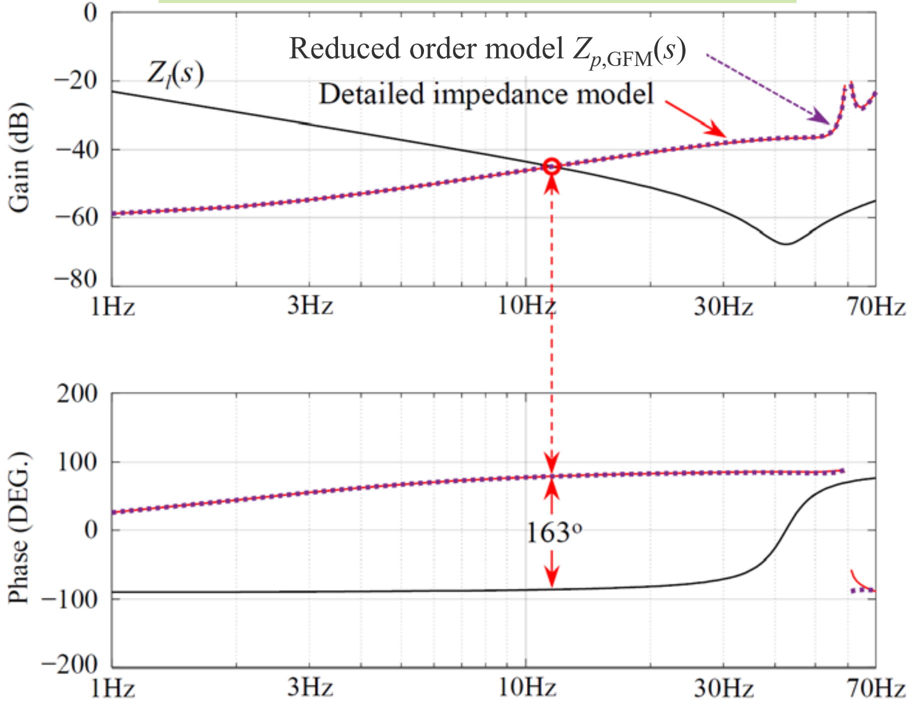

Summary

- Grid-forming control of DFIG-based Type III wind turbines naturally provides positive damping at subsynchronous frequencies.
  - The behavior is validated by EMT simulations, experimental impedance measurements of a 2.5 MW wind turbine drivetrain, and sequence impedance modeling.
  - This study demonstrates that the risk of SSR between wind power plants with type III wind turbines and series-compensated transmission lines or HVDC converters is low when the wind turbines are operated in grid-forming mode.
- Future work: Impact of grid-forming control of type III wind turbines on the risk of other types of subsynchronous oscillations (SSCI, SSTI, etc.) requires further evaluation.

Reference

- IEEE PES WindSSO Taskforce, “PES TR-80: Wind energy systems sub-synchronous oscillations: events and modeling, 2020,” https://resourcecenter.ieee-pes.org/publications/technical-reports/PES_TP_TR80_AMPS_WSSO_070920.html.
- Y. Cheng, L. Fan, J. Rose, and et al, “Real-world subsynchronous oscillation events in power grids with high penetrations of inverter-based resources,” IEEE Trans. on Power Systems, early access, Mar. 2022.
- L. Fan and Z. Miao, “Nyquist-stability-criterion-based SSR explanation for type-3 wind generators,” IEEE Trans. on Energy Conv., vol. 32, no. 3, pp. 807–809, Sep. 2012.
- S. Shah, V. Gevorgian, and H. Liu, “Impedance-based prediction of SSRgenerated harmonics in doubly-fed induction generators,” In Proc. IEEE Power & Energy Soc. Gen. Meeting, 2019, pp. 1–5.
- W. Yan, S. Shah, V. Gevorgian, and D. W. Gao, “Sequence impedance modeling of grid-forming inverters,” In Proc. IEEE Power & Energy Soc. Gen. Meeting, 2021, pp. 1–5.
- V. Gevorgian, S. Shah, W. Yan, and G. Henderson, “Grid-forming wind: getting ready for prime time, with or without inverters,” IEEE Electrifi. Mag., vol. 10, no. 1, pp. 52–64, Mar. 2022.
- V. Gevorgian, S. Shah, W. Yan , and et al, “Grid forming wind power,” presented at the ESIG Spring Techn. Workshop, Tucson, AZ, Mar. 21–24, 2022.
- S. Shah and V. Gevorgian, “Control, operation, and stability characteristics of grid-forming type III wind turbines,” presented at the Wind Integration Workshop, Nov. 11-12, 2020.
- W. Yan, L. Cheng, S. Yan, W. Gao and D. W. Gao, "Enabling and Evaluation of Inertial Control for PMSG-WTG Using Synchronverter With Multiple Virtual Rotating Masses in Microgrid," in IEEE Transactions on Sustainable Energy, vol. 11, no. 2, pp. 1078-1088, April 2020.

Thank you!

www.nrel.gov

Weihang.Yan@nrel.gov
Shahil.Shah@nrel.gov

NREL/PR-5D00-84326

This work was authored by Alliance for Sustainable Energy, LLC, the manager and operator of the National Renewable Energy Laboratory, operated by Alliance for Sustainable Energy, LLC, for the U.S. Department of Energy (DOE) under Contract No. DE-AC36-08GO28308. Funding provided by U.S. Department of Energy Office of Energy Efficiency and Renewable Energy Wind Energy Technologies Office. The views expressed in the article do not necessarily represent the views of the DOE or the U.S. Government.

NREL Transforming ENERGY